

Design of a biped robot actuated by pneumatic artificial muscles

Yixiang Liu, Xizhe Zang*, Xinyu Liu and Lin Wang

State Key Laboratory of Robotics and System, Harbin Institute of Technology, 150080, Harbin, Heilongjiang Province, China

Abstract. High compliant legs are essential for the efficient versatile locomotion and shock absorbency of humans. This study proposes a biped robot actuated by pneumatic artificial muscles to mimic human locomotion. On the basis of the musculoskeletal architecture of human lower limbs, each leg of the biped robot is modeled as a system of three segments, namely, hip joint, knee joint, and ankle joint, and eleven muscles, including both monoarticular and biarticular muscles. Each rotational joint is driven by a pair of antagonistic muscles, enabling joint compliance to be tuned by operating the pressure inside the muscles. Biarticular muscles play an important role in transferring power between joints. Walking simulations verify that biarticular muscles contribute to joint compliance and can absorb impact energy when the robot makes an impact upon ground contact.

Keywords: Biped robot, compliance, pneumatic artificial muscles, biarticular muscles

1. Introduction

Biped robots have the ability to walk, jump, and/or run, and have thus been a fascinating hotspot of research for many years because of their resemblance to human beings. Bipedal locomotion is an easy task for healthy humans, yet it remains an enormous challenge for biped robots. To date, numerous biped walkers have been designed and built to study and realize human-like walking.

The most conventional way to achieve biped walking is an approach based on zero-moment point (ZMP). In this approach, joint trajectories of the simplified robot model are predetermined on the basis of ZMP criteria to maintain dynamic balance during locomotion. A position-based controller commonly used on industrial robots is then applied to track the trajectories. The errors caused by model error and environment disturbance are eliminated utilizing posture balance algorithm [1]. Due to high-performance trajectory tracking of electrical motors, many humanoid robots are capable of stable walking and running [2, 3]. However, these robots tend to be energetically inefficient and brittle against terrain disturbance.

To solve the problems of high energy consumption and stilted gait, McGeer proposed the concept of “passive dynamic walking” as an alternative approach toward efficient and natural walking [4]. The

* Address for correspondence: Xizhe Zang, State Key Laboratory of Robotics and System, Harbin Institute of Technology, 150080, Harbin, Heilongjiang Province, China. Tel.: +86-045186413382; Fax: +86-045186414538; E-mail: zangxizhe@hit.edu.cn.

remarkable characteristic of a passive dynamic walking robot is its ability to settle into a natural gait on a downhill slope through the passive interaction of gravity and inertia [5]. Nevertheless, the walking behavior cannot be controlled because it is dominated by the fixed body dynamics [6]. To gain controllability, minimal actuation and control are added to passive dynamic walking robots to create “quasi-passive dynamic walking robots” [7]. Many quasi-passive dynamic walking robots, which can walk on flat terrains and even up small slopes, adopt electric motors to generate desired torque precisely [8], thus sacrificing the compliance and passiveness of joints [9].

The McKibben pneumatic artificial muscle is a suitable actuator to build powered passive dynamic walking robots and performs similarly to a biological muscle [10]. It has high compliance and can provide large force with a lightweight mechanism. Wisse, et al. built several biped robots with McKibben muscle actuators to walk on a flat floor, namely, Mike [11, 12], Max [13], and Denise [14]. Hosoda and his research group also developed a series of pneumatic actuated biped robots [15-23]. In spite of the complex characteristics of artificial muscles, such as nonlinearity, hysteresis, and time delay, these robots can walk stably by employing a simple limit-cycle controller without formally dealing with their complicated dynamics.

In this study, a biped robot actuated by pneumatic artificial muscles based on the musculoskeletal architecture of human lower limbs is proposed. A significant characteristic of the proposed biped robot is it incorporates both monoarticular muscles in a flexor-extensor configuration and biarticular muscles that span two joints. The joint compliance of the biped robot can be tuned by operating the pressure inside the muscles, which can help the robot increase energy efficiency and realize natural motions. What's more, collisions between the foot and ground will affect walking stability and reduce energy efficiency when a robot walks. Biarticular muscles allow work to be transferred between joints by coupling joint motions together [24, 25]. We believe they contribute to joint compliance of the biped robot and can absorb impact energy during touchdown. Walking simulations are carried out to verify the shock absorbency of different robot models.

The rest of this paper is organized as follows. Section 2 introduces the main design idea and properties of the biped robot. Section 3 presents the design of the biped robot. Section 4 introduces the kinematic analysis and discusses the simulation process and results, which demonstrate the impact energy absorbability of the biped robot using biarticular muscles. Section 5 provides the conclusion and discussion.

2. Key properties of the biped robot

2.1. Distribution of degrees of freedom

The lower limb of humans consists of pelvis, thigh, shank, and foot, interconnected by hip, knee, and ankle joint. Assuming joint translation is negligible, the hip joint can be modeled as a ball-and-socket joint with three degrees of freedom (DOF). The knee joint, as the most complicated joint in the human body, is usually simplified as a hinge joint with only one DOF around the pitch axis. The ankle joint, modeled as a universal joint, possesses two DOF for flexion/extension and abduction/adduction. It plays an important role in helping humans maintain balance during movement.

A main design idea behind the biped robot is to mimic the human walking gait with minimal DOF. Human walking is the coupling movement of walking in the sagittal plane and oscillating in the lateral plane. As the simplest bipedal walking model, biped robots that have two straight legs with rigidly connected arc-shaped feet, can achieve planar walking with hip joint actuation around the pitch axis.

However, they cannot bend their legs without knee joints and stand on the ground with circular feet. To overcome these problems, knee joints and flat feet with elasticity and viscosity at the ankle joints should be added. Consequently, human-like walking can be realized better in the sagittal plane with the three DOF around the pitch axis. In addition, the ankle roll motion is needed to stabilize the biped robot in the lateral plane and thus expand 2-D walking to 3-D walking.

Accordingly, the proposed biped robot has two three-segmented legs connected by the pelvis. Each leg is composed of thigh, shank, and flat foot. Both the hip joint and the knee joint have only one DOF around the pitch axis, while the ankle joint has two DOF around the roll and pitch axes. The biped robot has a total of eight internal DOF.

2.2. Arrangement of muscles

The muscle structure of human legs incorporates both monoarticular and biarticular muscles. Monoarticular muscles, which can only pull, mainly act as unidirectional force generators. To realize bidirectional motion, two monoarticular muscles are arranged in the flexor-extensor form. Biarticular muscles that span two joints play a crucial role in human walking. They are capable of transferring energy between joints by coupling joint motions. The leg can also absorb impact energy at ground contact.

The biped robot is designed based on the principles of human leg muscle architecture. As shown in Figure 1, each leg is simplified as a model that contains eleven major muscle groups, including eight monoarticular muscles and three biarticular muscles, each of which represents groups of synergist muscles across the joints. Consequently, the biped robot is a flexible and coordinative redundant system,

Monoarticular muscles on the hip joint include gluteus maximus, which extends the hip, and iliacus, which flexes the hip. Vastus lateralis extends the knee joint, and biceps femoris flexes the knee joint. The ankle joint is extended by soleus and flexed by tibialis anterior. Peroneus and ankle adductor are utilized for ankle abduction and adduction respectively. Biarticular muscles include rectus femoris and hamstring muscle, which both span the hip and knee joint, as well as gastrocnemius, which span the knee and ankle joint.

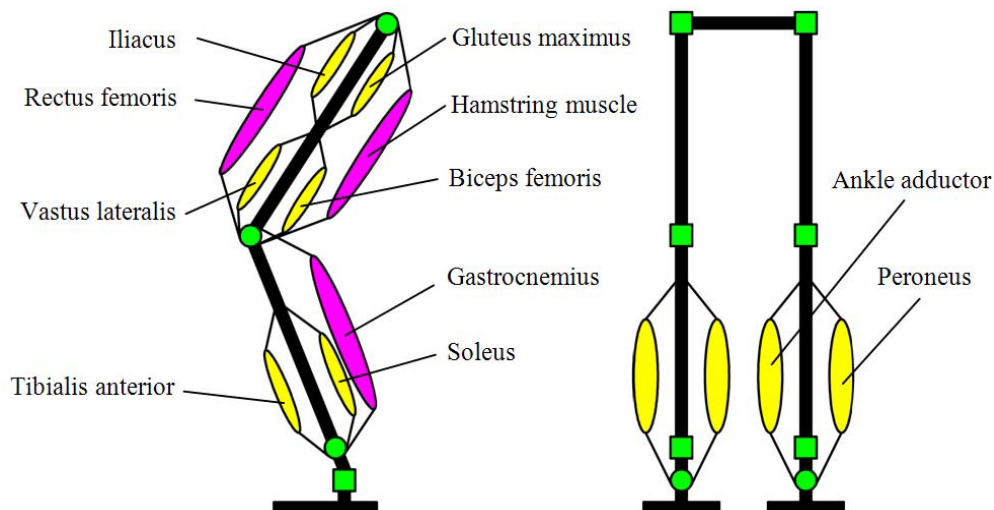


Fig. 1. Arrangement of muscles.

3. Design of the biped robot

3.1. Joint actuation with tunable compliance

A pneumatic artificial muscle with high compliance and high power–mass ratio is a suitable actuator owing to its similar characteristics in length–load curves with biological muscle. It consists of an inner rubber tube and an outer nylon sleeve, and contracts when compressed air is supplied to the inner tube. Two muscles have to be coupled antagonistically to have a bidirectional revolute joint because the muscles act only in tension and never in compression.

Figure 2(a) shows a common antagonistic joint drive mechanism. Two muscles are connected by wire rope winding on the pulley. In the initial state, both muscles are filled with a certain amount of air. When air is supplied into one muscle and expelled from the other one, the joint rotates to a specific angle. The forces of the muscles are in parallel form, which facilitates dynamic analysis. However, the wire rope drive results in unreliable factors. For example, if both muscles are relaxed, then the wire rope may separate from the pulley.

In this design, a different joint drive mechanism is adopted, as shown in Figure 2(b). The biggest characteristic of this configuration is that joint compliance can be tuned conveniently. When both muscles are supplied with some air and kept closed, a spring-like compliant joint is obtained because the muscles have elasticity. Changing the amount of air inside can regulate joint stiffness, enabling the joint to change its mode between passive and active. In the passive mode, both muscles are relaxed and the joint acts as a free rotational joint with minimal retarding force. In the active mode, the joint is capable of supplying the required torque for movement.

The structure of joint drive mechanism is illustrated in Figure 3, taking the hip joint as an example. The two hinge mounts are fixed on the pelvis and thigh respectively. Each end of the pneumatic artificial muscle is equipped with a connector, which is hinged with the hinge mount. The hip joint is driven to rotate by the two antagonistically arranged pneumatic muscles.

3.2. System overview

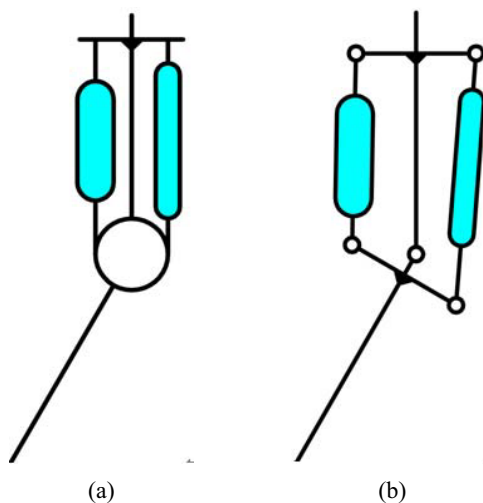


Fig. 2. Joint drive mechanisms.

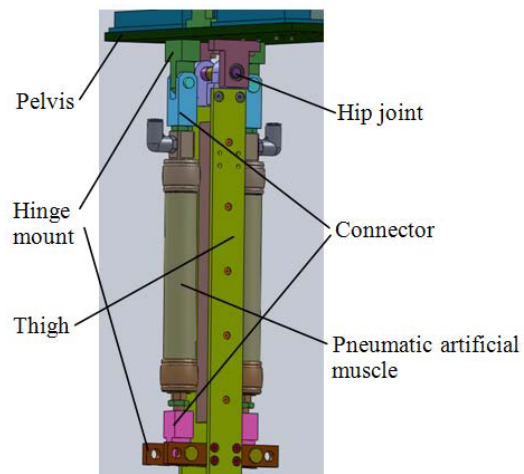


Fig. 3. Structure of joint drive mechanisms.



Fig. 4. Biped robot.

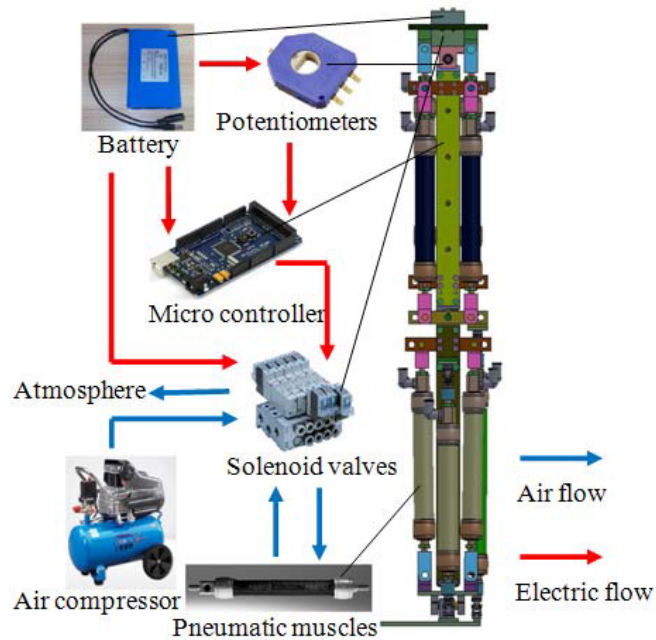


Fig. 5. System of the biped robot.

A musculoskeletal biped robot is designed in this study, as illustrated in Figure 4. The length of each link is expected to be of similar ratio as that of humans. The robot is 1100 mm high and 350 mm wide. The lengths of thigh and shank are 440 and 430 mm respectively. Mechanical stops are designed on the knee joints to avoid hyperextension. All the joints of the robot are driven by pneumatic artificial muscles produced by FESTO Corporation. The maximum contraction ratio of the muscles is approximately 25%. The muscle radius is 20 mm. Monoarticular muscles and biarticular muscles adopt two muscles with different relaxed lengths of 180 and 260 mm respectively. The force provided by the muscle is dependent on internal pressure and muscle deformation. The biped robot has a lightweight and flexible body because of the pneumatic artificial muscles. An on/off solenoid valve is selected to control the muscle because of its light weight and small size. It has three positions: supplying air to the valve, expelling air to the atmosphere and keeping closed.

The biped robot system illustrated in Figure 5 includes micro controller, lithium-ion battery, on/off solenoid valves, and potentiometers within its body. Compressed air is supplied to the valves from an external compressor via an air regulator. The micro controller sends operation commands, open or close, to the solenoid valves, and receives joint angles measured by the potentiometers.

4. Kinematic analysis and simulation of the biped robot

4.1. Kinematic analysis

Kinematic analysis is the theoretical foundation for designing the biped robot. For simplicity, the biped robot is restricted to motion in a plane. Figure 6 illustrates the kinematic analysis model, which has six DOF around the pitch axis. θ_i is the joint rotation angle, and L_1 and L_2 are the length of thigh and shank respectively.

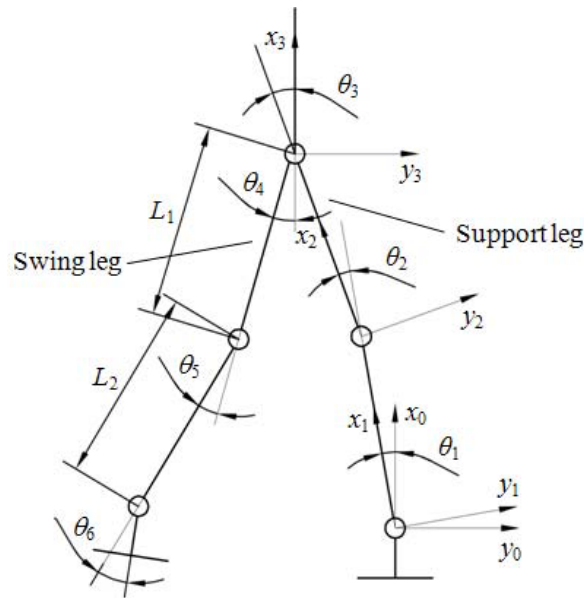


Fig. 6. Kinematic analysis model.

During walking, one leg acts as the support leg, while the other one acts as the swing leg. Considering that the two legs are symmetric, only analysis of the support leg is detailed. The swing leg can be analyzed in the same way. The base coordinate system is placed at the ankle joint and the hip joint is defined as the end point. Based on the homogeneous coordinate conversion, the position and pose of the end point in base coordinate can be presented as follows:

$$A_{Hip} = \begin{bmatrix} \cos(\theta_1 + \theta_2 - \theta_3) & \sin(\theta_1 + \theta_2 - \theta_3) & 0 & L_2 \cos \theta_1 + L_1 \cos(\theta_1 + \theta_2) \\ -\sin(\theta_1 + \theta_2 - \theta_3) & \cos(\theta_1 + \theta_2 - \theta_3) & 0 & -L_2 \sin \theta_1 - L_1 \sin(\theta_1 + \theta_2) \\ 0 & 0 & 1 & 0 \\ 0 & 0 & 0 & 1 \end{bmatrix}$$

Afterward, the inverse kinematic analysis is carried out. The position and pose of the end point are known and are indicated as

$$A_{Hip} = \begin{bmatrix} \cos \theta_H & \sin \theta_H & 0 & x_H \\ -\sin \theta_H & \cos \theta_H & 0 & y_H \\ 0 & 0 & 1 & 0 \\ 0 & 0 & 0 & 1 \end{bmatrix}$$

The joint variables are solved and written as

$$\theta_1 = \arctan \frac{x_H}{y_H} + \arctan \frac{L_2 + L_1 \cos \theta_2}{L_1 \sin \theta_2}$$

$$\theta_2 = \arccos \left(\frac{x_H^2 + y_H^2 - L_1^2 - L_2^2}{2L_1L_2} \right)$$

$$\theta_3 = \theta_H + \theta_1 + \theta_2$$

4.2. Simulation

Walking simulation of the biped robot is carried out to verify the feasibility of kinematic analysis and the shock absorbency of the biped robot. The walking pattern is generated using the ZMP based method. Given the walking parameters such as step length, step height, and cycle time etc., the trajectories of the hip joint and the foot of the swing leg are generated using polynomials respecting the continuity of position and velocity. Then joint angles are calculated utilizing inverse kinematics.

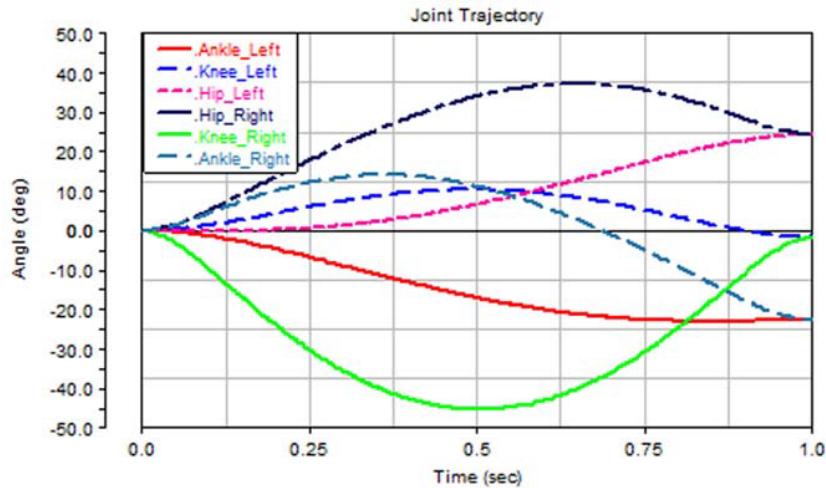


Fig. 7. Joint trajectories.

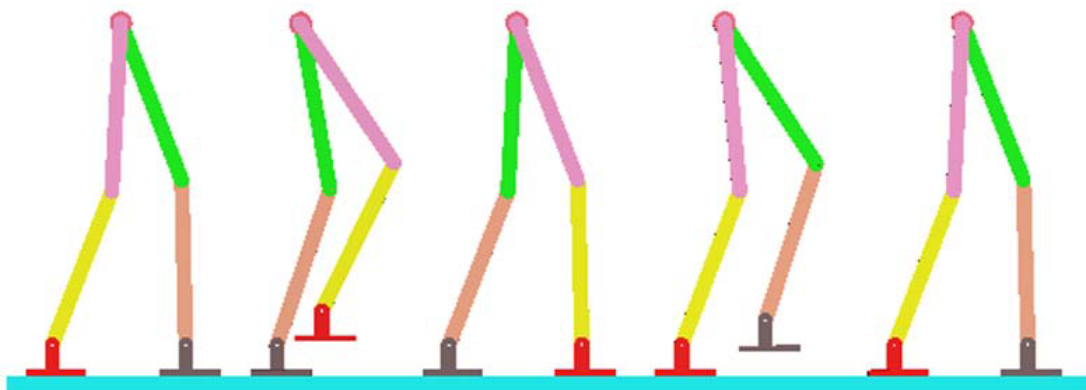


Fig. 8. Screenshots of walking.

The joint trajectories during a single step forward are shown in Figure 7. A PID controller is applied to each joint to track the desired trajectories. Figure 8 shows the screenshots of the realized walking in one cycle, which demonstrates the correctness of kinematic analysis.

Three simulation models are used to analyze the energy absorbability of the biped robot, as shown in Figure 9.

Model 1: All the joints are completely stiff actuated by motors.

Model 2: Each joint is actuated by a pair of monoarticular muscles.

Model 3: All the joints are actuated by three pairs of monoarticular muscles and three biarticular muscles.

Each robot model is controlled to walk according to the above walking simulation method. The value of ground reaction force (GRF) is obtained, as illustrated in Figure 10. The simulation results show that model 1 has the largest GRF among the three models, with a peak value that reaches 274 N. The force is so large that it may cause damage to the joint motors. The peak GRF of model 2 decreases drastically at 72.5 N because pneumatic artificial muscles have elasticity and behave like springs, helping the robot to absorb impact energy. Model 3 has the smallest peak GRF, which is about 1/10 of model 1 at only 29.2 N. These results confirmed our idea that biarticular muscles contribute to joint compliance and can absorb impact energy at ground contact.

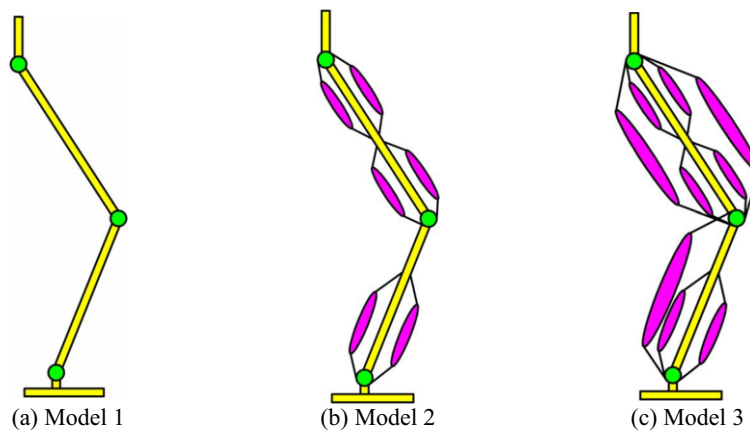


Fig. 9. Simulation models.

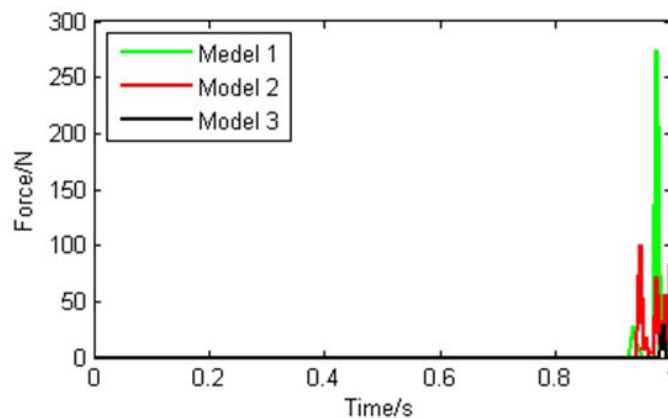


Fig. 10. Simulation results.

5. Conclusion and discussion

Human can perform efficient and versatile locomotion with compliant legs. In this study, a biped robot was designed based on the musculoskeletal architecture of human lower limbs. With the robot actuated by pneumatic artificial muscles, joint compliance could be tuned by operating the air pressure inside the muscles. The role of biarticular muscles was also studied. Through simulation, we demonstrated that biarticular muscles can help the biped robot absorb impact energy at ground contact during walking.

In the future, we aim to design a control system and realize human-like walking using this robot.

Acknowledgment

The work reported in this paper is supported by National Natural Science Foundation of China (grant 60905049) and the project of the State Key Laboratory of Robotics and System (grant SKLRS201304B).

References

- [1] M. Vukobratovic and B. Borovac, Zero-moment point-thirty five years of its life, *International Journal of Humanoid Robot* **1** (2004), 157–173.
- [2] S. Kajita, K. Kaneko, M. Morisawa, S. Nakaoka and H. Hirukawa, ZMP-based biped running enhanced by toe springs, *Proceedings of the 2009 IEEE International Conference on Robotics and Automation*, Roma, Italy, 2007, pp. 3963–3969.
- [3] S. Kim, C.H. Kim, B. You and S. Oh, Stable whole-body motion generation for humanoid robots to imitate human motions, *Proceedings of the 2009 IEEE/RSJ International Conference on Intelligent Robots and Systems*, St. Louis, USA, 2009, pp. 2518–2524.
- [4] T. McGeer, Passive walking with knees, *Proceedings of the 1990 IEEE International Conference on Robotics and Automation*, Cincinnati, 1990, pp. 1640–1645.
- [5] S.H. Collins, M. Wisse and A. Ruina, A three-dimensional passive-dynamic walking robot with two legs and knees, *International Journal of Robotics Research* **20** (2001), 607–615.
- [6] M. Garcia, A. Chatterjee and A. Ruina, Speed, efficiency, and stability of small-slope passive dynamic bipedal walking, *Proceedings of the 1998 IEEE International Conference on Robotics and Automation*, Leuven, Belgium, 1998, pp. 2351–2356.
- [7] M. Wisse, G. Feliksdaal, J.V. Frankenhuyzen and B. Moyer, Passive-based walking robot—Denise, a simple, efficient, and lightweight biped, *IEEE Robotics & Automation Magazine* **14** (2007), 52–62.
- [8] R. Tedrake, T.W. Zhang, M. Fong and H.S. Seung, Actuating a simple 3D passive dynamic walker, *Proceedings of the 2004 IEEE International Conference on Robotics and Automation*, New Orleans, LA, 2004, pp. 4656–4661.
- [9] S.O. Anderson, M. Wisse, C.G. Atkeson, J.K. Hodgins, G.J. Zeglin and B. Moyer, Powered bipeds based on passive dynamic principles, *Proceedings of 2005 5th IEEE-RAS International Conference on Humanoid Robots*, Tsukuba, Japan, 2005, pp. 110–116.
- [10] E. Kerasidi, G. Andrikopoulos, G. Nikolakopoulos and S. Manesis, A survey on pneumatic muscle actuators modeling, *Proceedings of the 2011 IEEE International Symposium on Industrial Electronics*, Gdansk, Poland, 2011, pp. 1263–1269.
- [11] M. Wisse and J. van Frankenhuyzen, Design and construction of MIKE: A 2D autonomous biped based on passive dynamic walking, in: *Adaptive Motion of Animals and Machines*, Hiroshi Kimura, Kazuo Tsuchiya, Akio Ishiguro, Hartmut Witte, eds., Springer Tokyo, Japan, 2006, pp. 143–154.
- [12] M. Wisse, Arend L. Schwab, Richard Q. van der Linde and Frans C. T. van der Helm, How to keep from falling forward: elementary swing leg action for passive dynamic walkers, *IEEE Transactions on Robotics* **21** (2005), 393–401.
- [13] M. Wisse, D.G.E. Hobbelen and A.L. Schwab, Adding an upper body to passive dynamic walking robots by means of a bisecting hip mechanism, *IEEE Transactions on Robotics* **23**(2007), 112–123.

- [14] M. Wisse, Three additions to passive dynamic walking: Actuation, an upper body, and 3D stability, Proceedings of the 2004 IEEE International Conference on Humanoid Robots, New York, NJ, USA, 2004, pp. 113–132.
- [15] T. Takuma and K. Hosoda, Controlling the walking period of a pneumatic muscle walker, *The International Journal of Robotics Research* **25** (2006), 861–866.
- [16] K. Hosoda, T. Takuma and A. Nakamoto, Design and control of 2D biped that can walk and run with pneumatic artificial muscles, Proceedings of the 2006 IEEE International Conference on Humanoid Robots, Genoa, Italy, 2006, pp. 284–289.
- [17] T. Takuma and K. Hosoda, Controlling walking behavior of passive dynamic walker utilizing passive joint compliance, Proceedings of the 2007 IEEE/RSJ International Conference on Intelligent Robots and Systems, San Diego, CA, USA, 2007, pp. 2975–2980.
- [18] K. Hosoda and K. Narioka, Synergistic 3D limit cycle walking of an anthropomorphic biped robot, Proceedings of the 2007 IEEE/RSJ International Conference on Intelligent Robots and Systems, San Diego, CA, USA, 2007, pp. 470–475.
- [19] K. Hosoda, T. Takuma, A. Nakamoto and S. Hayashi, Biped robot design powered by antagonistic pneumatic actuators for multi-modal locomotion, *Robotics and Autonomous Systems* **56** (2008), 46–53.
- [20] K. Narioka and K. Hosoda, Designing synergistic walking of a whole-body humanoid driven by pneumatic artificial muscles: An empirical study, *Advanced Robotics* **22** (2008), 1107–1123.
- [21] K. Narioka, S. Tsugawa and K. Hosoda, 3D limit cycle walking of musculoskeletal humanoid robot with flat feet, Proceedings of the 2009 IEEE/RSJ International Conference on Intelligent Robots and Systems, St. Louis, USA, 2009, pp. 4676–4681.
- [22] K. Ogawa, K. Narioka and K. Hosoda, Development of whole-body humanoid “Pneumat-BS” with pneumatic musculoskeletal system, In Proceedings of the 2011 IEEE/RSJ International Conference on Intelligent Robots and Systems, San Francisco, CA, USA, 2011, pp. 4838–4843.
- [23] K. Narioka, T. Homma and K. Hosoda, Humanlike ankle-foot complex for a biped robot, Proceedings of the 2012 12th IEEE-RAS International Conference on Humanoid Robots, Osaka, Japan, 2012, pp. 15–20.
- [24] M.A. Lewis and T.J. Klein, A robotic biarticulate leg model, Proceedings of the 2008 IEEE Biomedical Circuits and Systems Conference, Baltimore, MD, USA, 2008, pp. 57–60.
- [25] T.J. Klein and M.A. Lewis, A robot leg based on mammalian muscle architecture, Proceedings of the 2009 IEEE International Conference on Robotics and Biomimetics, Guilin, China, 2009, pp. 2521–2526.